



## Sol-Gel-Derived Hybrid Coatings for Corrosion Protection

T.P. CHOU

*Department of Materials Science and Engineering, University of Washington, Seattle, WA, USA*

C. CHANDRASEKARAN

*Boston Scientific Corporation, Redmond, WA, USA*

G.Z. CAO\*

*Department of Materials Science and Engineering, University of Washington, Seattle, WA, USA*

gzcao@u.washington.edu

**Abstract.** The corrosion resistance of sol-gel-derived, organic-inorganic, silica-based hybrid coatings was studied. Hybrid sols were prepared by copolymerizing tetraethylorthosilicate (TEOS) and 3-methacryloxypropyltrimethoxysilane (MPS) with a two-step acid-catalyst process. Hybrid coatings were dip-coated on 304 and 316 stainless steel substrates and annealed at 300°C for 30 minutes. The adhesion, flexibility, and biocompatibility of the coatings were examined. Hybrid coatings were found to be relatively dense, uniform and defect free. Electrochemical analyses showed that the coatings provided excellent corrosion protection by forming a physical barrier, which effectively separated the anode from the cathode. In addition, further experimental results revealed that the corrosion patterns are strongly dependent on the nature of the stainless steel substrates. Some possible mechanisms for corrosion breakdown associated with each type of substrate are also introduced.

**Keywords:** sol-gel processing, hybrid coatings, organic-inorganic coatings, corrosion protection, stainless steel

### Introduction

A generic approach to enhance corrosion resistance is to apply protective films or coatings. Through the modification of the chemical composition of the coatings, such protective coatings can also permit the introduction of other desired chemical and physical properties, such as mechanical strength and hydrophobicity. Various organic coatings have been studied for corrosion protection [1–3]. Various oxide coatings by sol-gel processing have been studied extensively for corrosion protection of stainless steel [4–8]. In spite of all the advantages of sol-gel processing, sol-gel oxide coatings suffer from several drawbacks. Specifically, the high annealing or sintering temperatures (>800°C) required to achieve a dense microstructure could possibly

introduce cracks and/or delamination within the sol-gel coatings [9–12].

One viable approach to dense, sol-gel-derived coatings without post-deposition annealing at elevated temperatures is to synthesize organic-inorganic hybrid coatings. Relatively dense organic-inorganic hybrid coatings have been developed for applications, including wear resistance [13, 14] and corrosion protection [15–17]. In this paper, we studied the corrosion resistance of sol-gel-derived, organic-inorganic hybrid coatings on two types of stainless steel. The current research was also aimed at developing corrosion protecting sol-gel coatings with desired flexibility and biocompatibility. It was demonstrated that sol-gel-derived hybrid coatings could significantly enhance the corrosion protection of stainless steel substrates. Corrosion resistance of multiple coatings, flexibility, and adhesion were discussed and

\*To whom all correspondence should be addressed.

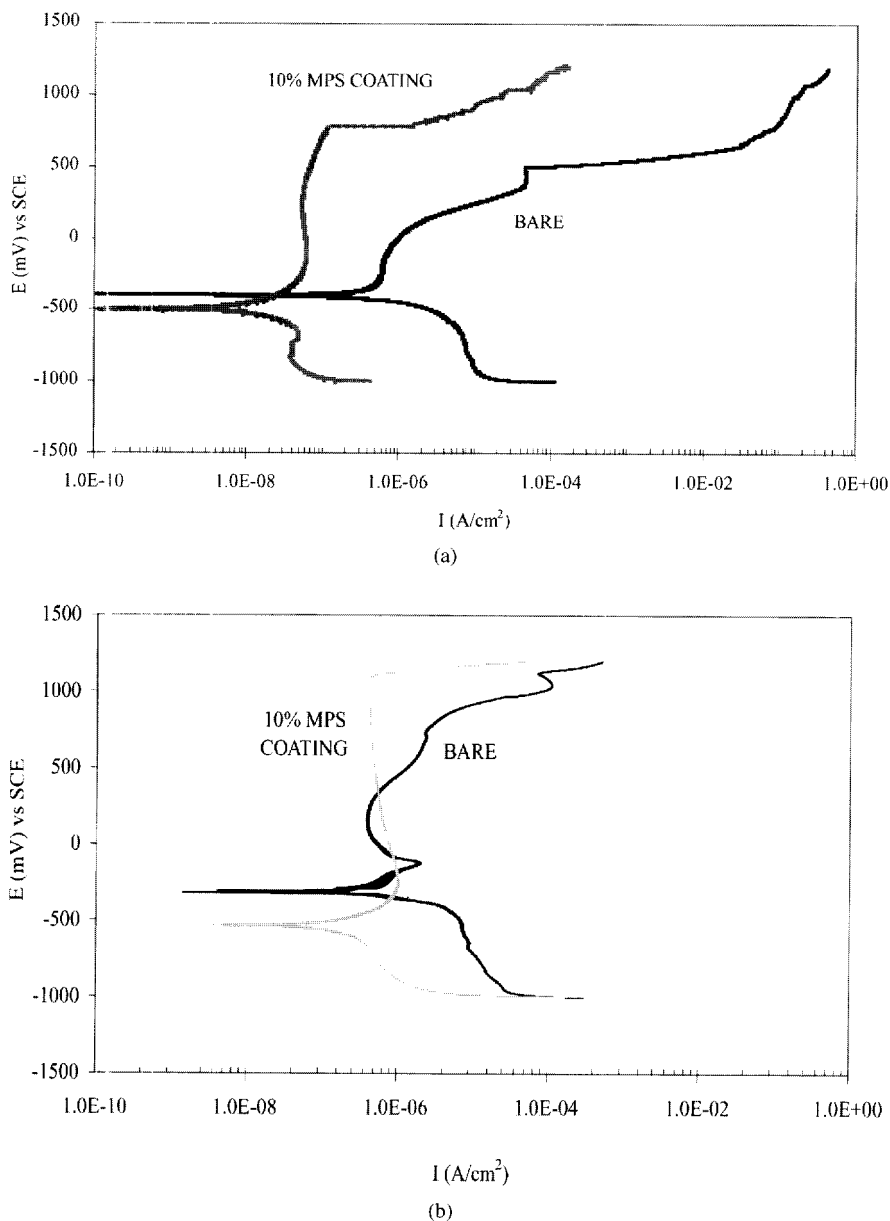


Figure 1. Polarization curves of bare and 10% MPS sol-gel coated (a) 304 stainless steel substrates and (b) 316 stainless steel substrates.

efforts were made to understand possible failure mechanisms.

### Experimental

The 304 and 316 stainless steel substrates used for the analysis of the sol-gel coatings had been electropolished and exposed to surface hydroxylation at an elevated temperature to ensure a tight bond and good

adhesion between the substrate surface and the sol-gel coating [18]. The silica-based, organic-inorganic hybrid sol was prepared with an acid-catalyzed, two-step hydrolysis-condensation process. The hybrid sol was prepared by admixing a silica precursor, tetraethylorthosilicate (TEOS,  $\text{Si}(\text{OC}_2\text{H}_5)_4$ ), and an organic precursor, 3-methacryloxypropyltrimethoxysilane (MPS,  $\text{H}_2\text{CC}(\text{CH}_3)\text{CO}_2(\text{CH}_2)_3\text{Si}(\text{OCH}_3)_3$ ), to control the flexibility and density of the sol-gel network. After

Figure 2. Polarization curves of bare and 10% MPS sol-gel coated 304 stainless steel substrates with different coating thicknesses.

substrate preparation, the sol was dip-coated on the substrate. The coating thickness was controlled by the dip-coating time in the sol at a fixed withdrawal rate. The coated substrates were dried in the sol for 24 hours at room temperature. The same coating procedure was used for the same coating thickness. The coated substrates were stored in a desiccator for approximately 15 months before use. The substrates were stored in a desiccator for approximately 15 months before use. The substrates were stored in a desiccator for approximately 15 months before use.

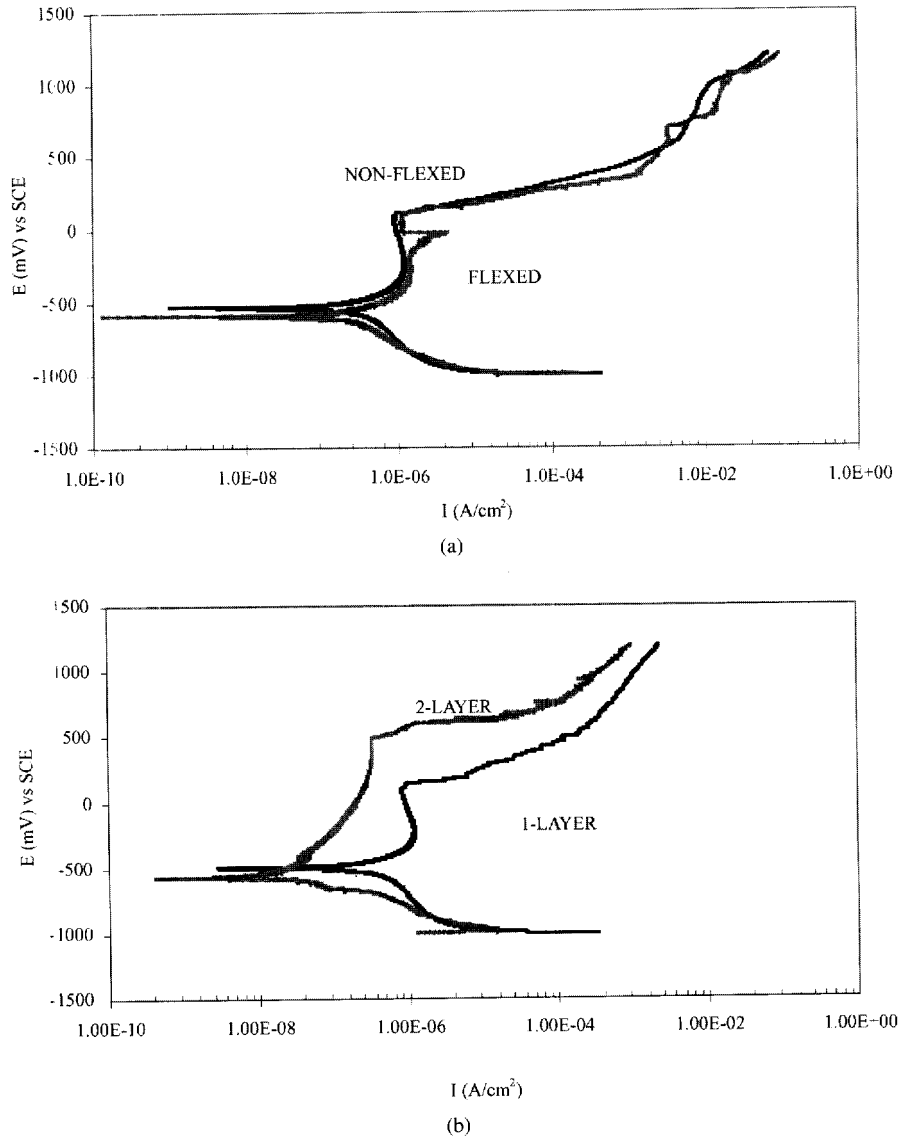
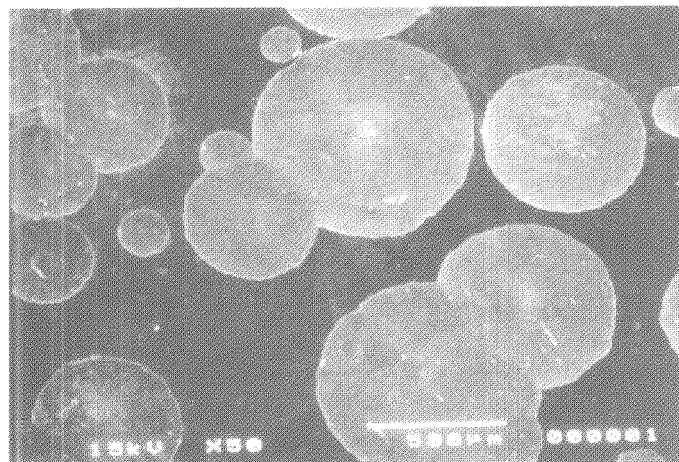


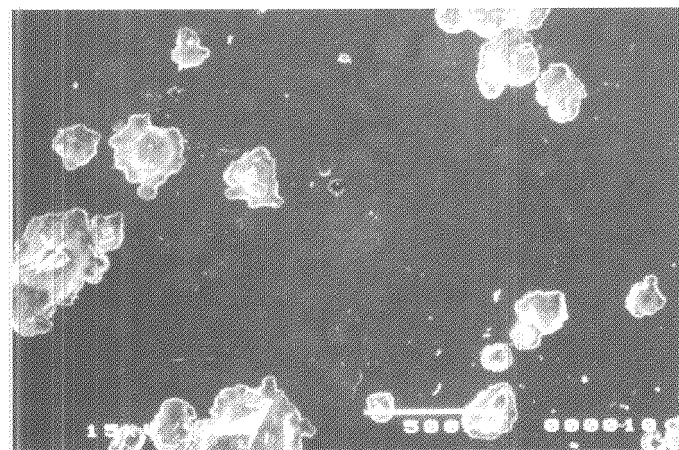
Figure 2. Polarization curves of (a) non-flexed and flexed 304 stainless steel substrates with 10% MPS sol-gel coating and (b) 304 stainless steel substrates with 1-layer and 2-layer 10% MPS sol-gel coating.

substrate preparation and sol preparation, film deposition of the coating onto the substrates utilized a simple dip-coating process. The substrates were dipped in the sol at a constant rate of 14 cm/min, immersed in the sol for approximately 1 minute, withdrawn at the same constant rate, and then air-dried for approximately 15 minutes. Following deposition, the substrates were sintered at 300°C for 30 minutes at a heating and cooling rate of 5°C/min to ensure densification of the gel network. A detailed study was focused on sol-gel coatings with a TEOS:MPS ratio of 90:10.

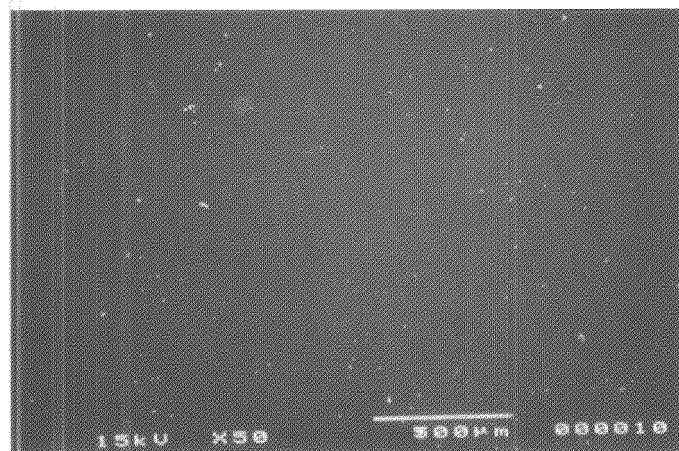
Polarization measurements were carried out potentiodynamically at room temperature under extreme environmental conditions consisting of an aqueous, air-exposed, saturated sodium chloride (32% NaCl) solution, a saturated calomel reference electrode (SCE), and a platinum counter electrode. All potentiodynamic measurements were performed within the range of -1000 mV to 1200 mV versus SCE at a rate of 2 mV/s. Optical Microscopy and scanning electron microscopy (SEM) were also performed on the substrates to characterize the surface morphology. In



(a)



(b)



(c)

Figure 3. SEM images of (a) a bare stainless steel substrate, (b) a 10% MPS sol-gel coated 304 stainless steel substrate, and (c) a 10% MPS sol-gel coated 316 stainless steel substrate after corrosion pitting from polarization analysis.

addition, bioe  
means of cyto

### Results and D

Optical micro  
uniform, homo  
coatings on st  
tained prior to  
300°C for 30 m  
indicated that  
mately 200 nm

Figure 1(a) a  
of both bare an

Figure 4. Schemati  
304 stainless steel su

addition, biocompatibility tests were characterized by means of cytotoxicity and hemolysis.

### Results and Discussion

Optical microscopy and SEM analyses revealed that uniform, homogeneous, and crack-free hybrid sol-gel coatings on stainless steel substrates were readily obtained prior to and after post-deposition annealing at 300°C for 30 minutes. Ellipsometry measurements also indicated that a uniform coating thickness of approximately 200 nm was deposited on the substrates.

Figure 1(a) and (b) compares the polarization curves of both bare and 10% MPS sol-gel coated 304 and 316

stainless steel substrates. A passivation region with a rather low passivation current density implied that the sol-gel coating indeed provided a physical barrier for blocking the electrochemical process. The polarization curves of the sol-gel coated substrates was appreciably different from that of the bare stainless steel substrates indicating that the hybrid coating had an effect on the corrosion behavior. In addition, a distinct passivation region was present for the coated substrates, whereas, no definitive passivation region was found for the bare stainless steel substrates.

Figure 2(a) and (b) shows the flexibility and versatility of the sol-gel coating on 304 stainless substrates by comparing the polarization curves of 10% MPS coatings on stainless steel substrates. Figure 2(a) clearly

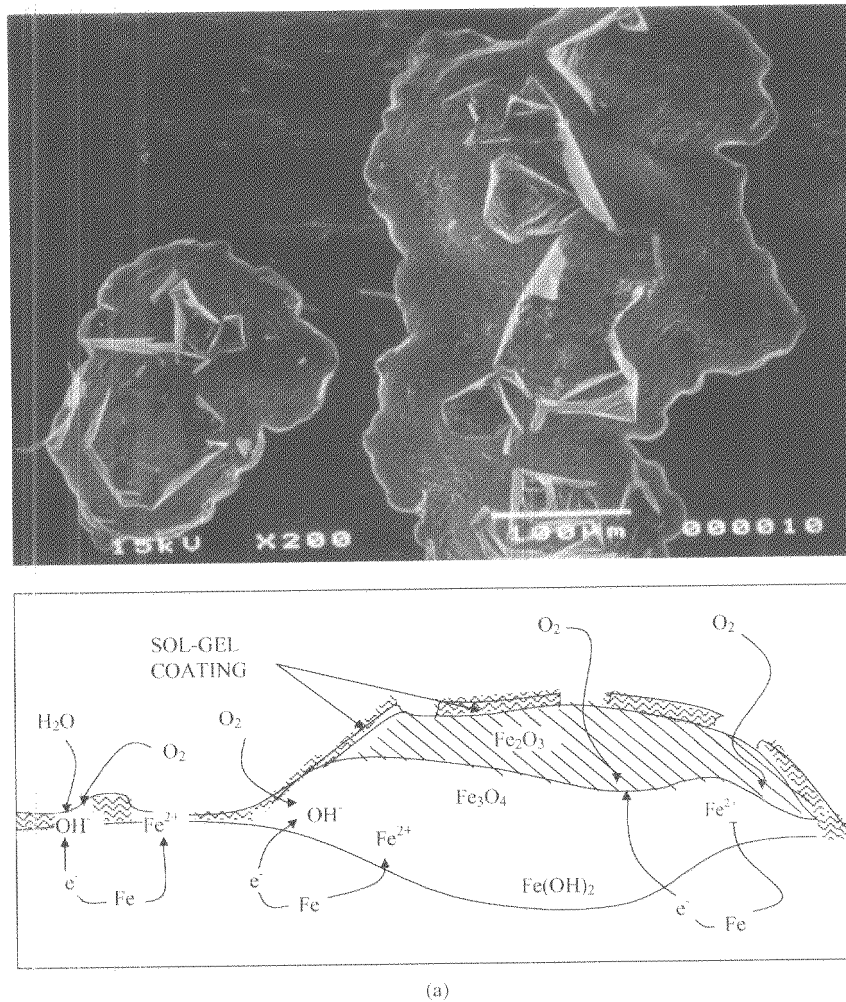
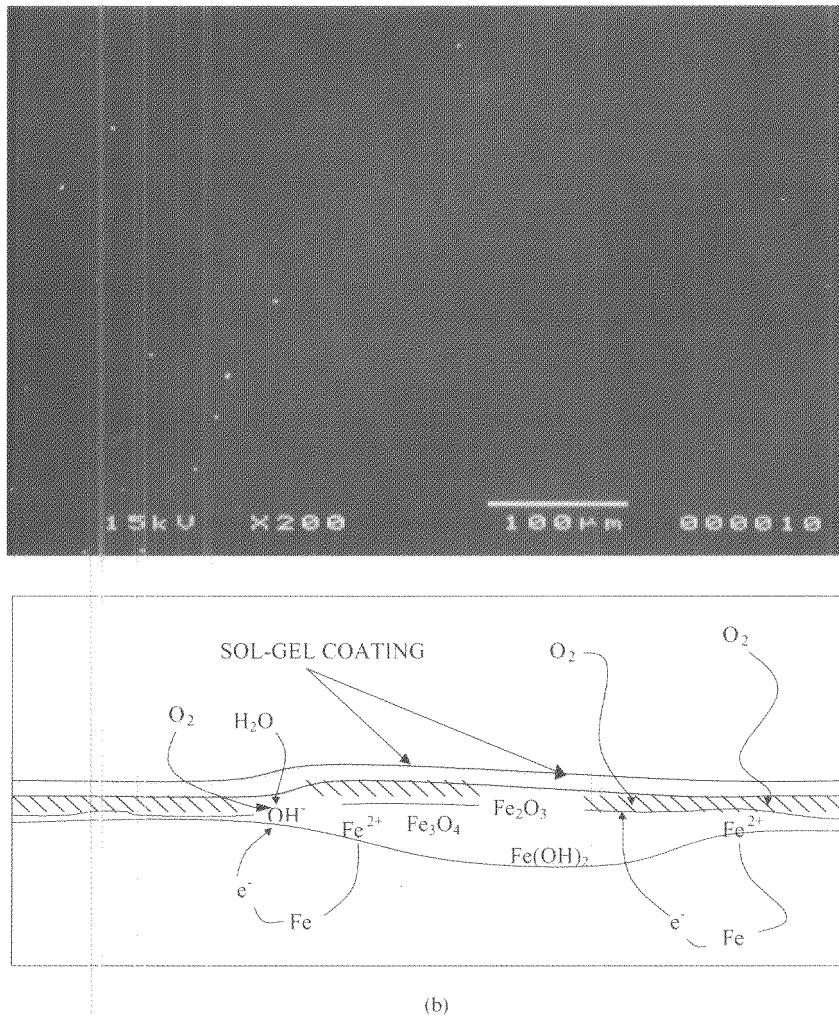


Figure 4. Schematic illustrations of possible corrosion mechanisms and their respective SEM images for (a) 10% MPS hybrid coating on a 304 stainless steel substrate and (b) 10% MPS hybrid coating on a 316 stainless steel substrate.

(Continued on next page.)



(b)

Figure 4. (Continued).

shows that the two polarization curves are identical, indicating that flexure had introduced neither cracking nor delamination in the hybrid coatings. Figure 2(b) compares the polarization curves of one-layer and two-layer coatings on 304 stainless steel. The two-layer coating demonstrated appreciably enhanced corrosion protection due to the reduced diffusion rate or conducting current density through the thicker coating. The higher potential of the passive region could be ascribed to the doubled thickness from the two-layer hybrid coating, which would be more resistive to induced interface corrosion failure.

Figures 3(a)–(c) compares the SEM images of the bare and 10% MPS sol-gel coated 304 and 316 stainless steel substrates after potentiodynamic polarization

tests. The extent of corrosion was appreciably different. The corrosion pits in the bare substrate are much larger than that in the sol-gel coated substrates. It was also found that the 304 stainless steel substrate with hybrid coating showed more extensive pitting from electrochemical reactions along the surface than the 316 stainless steel substrate. The delamination and breakdown of the coating on 304 stainless steel could be clearly seen along the edge and interior of the corrosion pits, indicating preferential localized attack after the electric potential exceeded the breakdown potential. The 316 stainless steel substrate with hybrid coating showed no signs of pitting along the surface, where no appreciable delamination or cracking of the coating was seen.

Figure 4(a) of the coated 304 stainless steel substrate, possible corrosion products, and possible corrosion products on the 304 stainless steel substrate. The chemical reactions occurring at the interface, delamination of the coating from the substrate, possible corrosion products at the interface [13]. The mechanism at the interface and the 316 stainless steel substrate that the electrochemical reactions and metal ions from the substrate result in a passive layer forming a passivation film with high resistance.

Some preliminary studies on the inorganic hybrid coatings showed good stability. Specific examples of the inorganic hybrid coatings were more than 99.99% (below 1000°C) coatings are corrosion resistant. The above results indicate that the hybrid coatings required, the hybrid coatings are compatible materials for various applications.

## Conclusions

Silica-based hybrid coatings by a step acid catalyzed sol-gel process form, defect-free coatings on stainless steel substrates. The corrosion protection provided by the hybrid coatings which effectively act as a cathode electrically. The corrosion protection could be improved by increasing the coating thickness. The surface corrosion products were removed by the sol-gel process.

Figure 4(a) and (b) shows the close-up SEM images of the coated 304 and 316 stainless steel substrates and possible corrosion mechanisms. Figure 4(a) depicts the possible corrosion mechanism of sol-gel coatings on the 304 stainless steel substrate. The localized electrochemical reaction at the interface resulted in debonding, delamination and lifting of the coating from the substrate, possibly due to hydrolysis reactions at the interface [13]. Figure 4(b) suggests a different corrosion mechanism at the interface between the sol-gel coating and the 316 stainless steel substrate. It is possible that the electrochemical reaction between the corrosive and metal ions at the interface of the coating and the substrate resulted in the formation of an oxide layer, forming a passivation layer to enhance the corrosion resistance.

Some preliminary tests showed that the organic-inorganic hybrid coatings possess good biocompatibility. Specifically, no cell lysis or intracytoplasmic granules were noted, which indicated that the organic-inorganic hybrid coatings are non-cytotoxic. Furthermore, the percent of cell lysis was determined to be 0.00% (below the detection limit), and thus the sol-gel coatings are considered to be non-hemolytic. Although the above results are preliminary and further testing is required, the biocompatibility test results are in good agreement with literature stating that SiO<sub>2</sub> is a biocompatible material [19, 20]. Thus, SiO<sub>2</sub>-MPS hybrid coatings are promising candidates for biocompatible applications.

## Conclusions

Silica-based hybrid coatings, prepared by a two-step acid catalyst sol-gel process, were found uniform, defect-free and relatively dense. Hybrid coatings on stainless steel substrates demonstrated enhanced corrosion protection by forming a physical barrier, which effectively separated the anode from the cathode electrically. It was found that the corrosion protection could be further enhanced with an increased coating thickness. SEM study suggested that interface corrosion is the likely mechanism of breakdown of the sol-gel coatings. The hybrid coatings

also demonstrated excellent adhesion and flexibility, which could be attributed to the formation of chemical bonding at the interface and the incorporation of organic components, respectively. In addition, preliminary experiments suggest that the hybrid coatings might have good biocompatibility for bio-medical applications.

## References

1. G. Grundmeier, W. Schmidt, and M. Stratmann, *Electrochimica Acta* **45**, 2515 (2000).
2. R. Haneda and K. Aramaki, *J. Electrochem. Soc.* **145**, 2786 (1998).
3. W. Lu, R.L. Elsenbaumer, T. Chen, and V.G. Kulkarni, *Mat. Res. Soc. Symp. Proc.* **488**, 653 (1998).
4. M. Guglielmi, *J. Sol-Gel Sci. Tech.* **1**, 177 (1994).
5. D.C.L. Vasconcelos, J.N. Carvalho, M. Mantel, and W.L. Vasconcelos, *J. Non-Cryst. Solids* **273**, 135 (2000).
6. M. Simoes, O.B.G. Assis, and L.A. Avaca, *J. Non-Cryst. Solids* **273**, 159 (2000).
7. M. Atik, S.H. Messaddeq, F.P. Luna, and M.A. Aegerter, *J. Mater. Sci. Lett.* **15**, 2051 (1996).
8. P. Neto, M. Atik, L.A. Avaca, and M.A. Aegerter, *J. Sol-Gel Sci. Tech.* **2**, 529 (1994).
9. C.J. Brinker and G.W. Scherer, *Sol-Gel Science: The Physics and Chemistry of Sol-Gel Processing* (Academic Press, San Diego, CA, 1990).
10. A.C. Pierre, *Introduction to Sol-Gel Processing* (Kluwer, Boston, MA, 1998).
11. L.F. Francis, *Mater. Manufacturing Process* **12**, 963 (1997).
12. X.H. Han, G.Z. Cao, T. Pratum, D.T. Schwartz, and B. Lutz, *J. Mater. Sci.* **36**, 985 (2001).
13. C.M. Chan, G.Z. Cao, H. Fong, M. Sarikaya, T. Robinson, and L. Nelson, *J. Mater. Res.* **15**, 148 (2000).
14. J. Wen and G.L. Wilkes, *J. Inorganic and Organometallic Polymers* **5**, 343 (1995).
15. J.S. Park and J.D. Mackenzie, *J. Amer. Ceram. Soc.* **78**, 2669 (1995).
16. S.H. Messaddeq, S.H. Pulcinelli, C.V. Santilli, A.C. Guastaldi, and Y. Messaddeq, *J. Non-Cryst. Solids* **247**, 164 (1999).
17. M. Atik, F.P. Luna, S.H. Messaddeq, and M.A. Aegerter, *J. Sol-Gel Sci. Tech.* **8**, 517 (1997).
18. T.P. Chou, C. Chandrasekaran, S.J. Limmer, S. Seraji, Y. Wu, M. Forbess, C. Nguyen, and G.Z. Cao, *J. Non-Cryst. Solids* **290**, 153 (2001).
19. L.L. Hench, *Sol-Gel Silica: Properties, Processing and Technology Transfer* (Noyes, Westwood, New Jersey, 1998).
20. R.K. Iler, *The Chemistry of Silica: Solubility, Polymerization, Colloid and Surface Properties, and Biochemistry* (John Wiley and Sons, New York, 1979).